Balancing Computation Speed and Quality: A Decentralized Motion Planning Method for Cooperative Lane Changes of Connected and Automated Vehicles

Bai Li ⓘ, *Student Member, IEEE*, Youmin Zhang ⓘ, *Senior Member, IEEE*, Yiheng Feng ⓘ, Yue Zhang ⓘ, *Student Member, IEEE*, Yuming Ge, and Zhijiang Shao

Abstract—This paper focuses on the multi-vehicle motion planning (MVMP) problem for cooperative lane changes of connected and automated vehicles (CAVs). The predominant decentralized MVMP methods can hardly explore and utilize the cooperation capability of a multi-vehicle team, thus they usually lead to low-quality solutions. This paper proposes a two-stage MVMP framework to find high-quality online solutions. Concretely, at stage 1, the CAV platoon transfers from its original formation to a sufficiently sparse formation; at stage 2, all the CAVs simultaneously change lanes with collision avoidance implicitly ensured. The CAVs only involve longitudinal rather than lateral motions at stage 1, thus the collision-avoidance constraints can be easily handled. Since stage 2 begins with a sparse formation, the implicitly ensured collision avoidance can be completely omitted then. Through this, the proposed method avoids directly handling the challenging collision avoidance conditions, thereby being able to compute fast. As the vehicles run cooperatively and simultaneously at either stage, the obtained solutions are near-optimal. The completeness, effectiveness, and quality of the proposed two-stage MVMP method are validated through theoretical analysis and comparative simulations.

Index Terms—Collision avoidance, connected and automated vehicles (CAVs), intelligent vehicles, lane change, motion planning, optimization method.

I. INTRODUCTION

A. Background and Motivations

THE incessant developments in connected and automated vehicles (CAVs) have brought significant benefits in promoting road capacity, enhancing mobility, and reducing fuel consumptions [1]. Research efforts on CAVs may include cooperative collision avoidance, platooning, and cooperative adaptive cruise control [2], which require the capabilities to generate cooperative driving behaviors. In a multi-CAV system, the decision-making unit is responsible for generating the desired cooperative motions for the CAVs, thus it largely determines the intelligence level of the whole system [3]. This study focuses on the multi-vehicle motion planning (MVMP) problem.

MVMP aims at computing safe, comfortable, and dynamically feasible paths/trajectories from the vehicles' current configurations to achieve specified terminal goals [4]. Nominally, an MVMP problem should be formulated in a centralized form. In solving a centralized MVMP problem, all the decision variables are determined simultaneously with all the constraints considered. However, a centralized MVMP problem is numerically intractable due to the geometrical scaling of computational complexity with the quantity of vehicles [5].

With the purpose of finding solutions in real time, the predominant MVMP methods do not handle *all* of the constraints simultaneously. Instead, they convert the centralized formulation into decentralized forms. Although the decentralized formulations are computationally simple, the solutions are usually conservative, i.e., far from being optimal [6], [7]. That is because the capability to interact and cooperate is highly limited by the applied decentralization strategies. At this point, the prevalent decentralized MVMP methods run fast at the sacrifice of solution quality. This limitation motivates the authors to develop a decentralized method which not only runs fast, but also maintains the inter-vehicle cooperation capabilities as much as possible.

Lane change is selected as the MVMP scenario in this work, because it is a basic and critical element of complex driving maneuvers such as overtaking, merging, exit, and emergency clearance [8], [9]. Improper lane change execution is a primary cause for car crashes worldwide [10]–[12]. In addition, a single vehicle in congested traffic often fails to change lane without collaborating with the surrounding vehicles [13]. Therefore, a well-designed MVMP method has great potentials in providing high-quality cooperative lane change motions for a multi-CAV team.

B. Related Works

Single-vehicle lane change motion planning methods have been studied extensively [4], [14], but most of them cannot be applied directly to tackle multi-vehicle cases. This section reviews the prevalent decentralized MVMP methods proposed for cooperative lane change schemes.

Luo *et al.* [15] described the lane change trajectories as parameterized quintic polynomials, and then calculated the parameters by solving a nonlinear programming (NLP) problem with safety, comfort, and travel efficiency considered. Fu *et al.* [16] also defined the lane-change trajectories as parameterized polynomials, and then sorted satisfactory solutions via differential evolution algorithm in the ordinal optimization framework. Atagoziyev *et al.* [17] categorized all the lane change scenarios into seven typical cases; in each case, only one vehicle has the lane change intention; the surrounding normal vehicles cooperatively adjust the formation until the central lane-change vehicle can change the lane safely; this single-vehicle lane change process continues sequentially if more than one vehicle intends to change lane. Similarly, Samiee *et al.* [18] developed a permission scope, whereby a lane change is not allowed until the current situation matches one of the four typically predefined scenarios, and the corresponding maneuvers are determined by human logics. Desiraju *et al.* [19] classified all the involved CAVs into multiple groups according to their target lanes, and then sequentially execute the lane changes in each group. Suh *et al.* [20] utilized a "lane change envelope" to isolate a lane-change vehicle from its neighbors; once the vehicle is not interfered by the others, lane change can be safely implemented. Li *et al.* [21] proposed a two-stage cooperative motion planner, wherein the platoon must be re-formulated as a homogeneous one at stage 1, then the corresponding off-line solution to such a standard problem is implemented directly at stage 2.

In handling cooperative lane change problems, the aforementioned decentralized MVMP algorithms share some typical drawbacks. Firstly, the kinematic capabilities of the CAVs are not fully exploited; instead, they are highly limited by specified types of path shapes [15], [16], [18], simple rules [17], and specified car-following principles [19]. These specification strategies can drastically reduce the computational complexity, but the chances to find high-quality solutions are lost at the same time. Secondly, the MVMP decisions are made *jointly* rather than *simultaneously* [7]. Only one vehicle can execute the lane change maneuvers at one time, while the other vehicles must keep their lanes. Since the vehicles' motions are not simultaneously
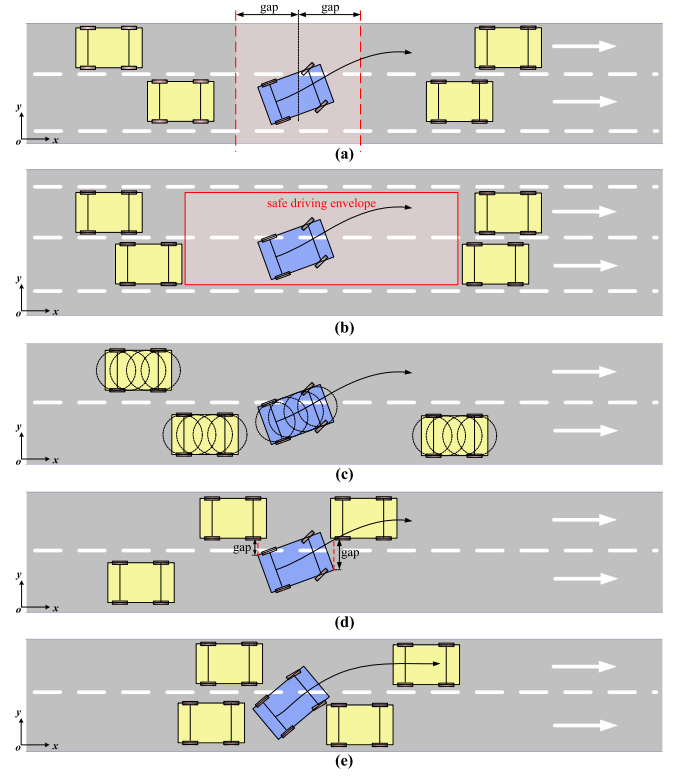

Fig. 1.   Schematics of various formulations of collision-avoidance constraints: (a) gap-based constraint, which requires the surrounding vehicles should not entering the highlighted region; (b) envelope-based constraint, which forbids the surrounding vehicles entering the highlighted box region; (c) circle based constraint, which uses multiple circles to represent a rectangle [16], [21]; (d) corner-gap based constraint, which requires gaps between the rectangle corners and the surroundings [18]; and (e) an example that fully utilizes road space.

computed, the cooperation capability is hardly explored and utilized. Thirdly, the collision-avoidance constraints are not precisely formulated. Some methods (e.g., [15], [17], [19]) used gaps to keep the lane-change vehicles from the through vehicles (Fig. 1(a)). Similarly, [20] associated a moving box with the lane-change vehicle to define the no-entrance region (Fig. 1(b)). The formulations in [16], [18], and [21] are less conservative (see Fig. 1(c) and (d), respectively), but none of them can achieve the delicate maneuvers as shown in Fig. 1(e), wherein the vehicles are making good use of the road space. Finally, if the decentralized algorithms are not complete, then additional recovery steps are needed to ensure deadlock-free and/or collision-free in some corner cases [15], [18]. A review of the prevalent studies is summarized in Table I.

C. Contributions

The highlights of this study are three-folded. Firstly, a two-stage decentralized MVMP method, which can address the issues listed in Table I, is proposed for cooperative lane changes in a CAV-only environment. Secondly, theoretical analysis is provided to verify the completeness of the proposed two-stage MVMP method. Thirdly, exhaustive simulations are carried out to show the advantages of the proposed method over the existing ones.

Reference / Key Performance Indicator	[15]	[16]	[17]	[18]	[19]	[20]	[21]	This Work
Lane change maneuvers are not limited to specified patterns.	×	×	N/A	×	×	×	√	√
Multiple vehicles can change lanes simultaneously.	×	×	×	×	√	×	√	√
Collision-avoidance constraints are precise.	×	√	×	√	×	×	√	√
Feasible solutions are always available.	×	√	√	×	√	√	√	√
Solutions are obtained in real time.	√	×	√	√	√	√	×	√
Can handle non-adjacent lane changes.	√	√	×	×	×	√	√	√

The rest of this paper is organized into the following sections. Section II states the nominal cooperative lane change scheme. Section III introduces the two-stage MVMP method. Simulation setups, results, and in-depth discusses are provided in Section IV. Section V concludes the paper.

II. PROBLEM STATEMENT

This section states the cooperative lane change MVMP scheme in the form of an optimal control problem, which consists of the vehicle kinematics-, scenario-, and task-related constraints, as well as the optimization objective. We assume that the vehicles travelling on the road are all CAVs, rather than disconnected or non-cooperative ones.

A. Kinematics-Based Constraints

To describe the CAV kinematics, Ackerman's bicycle model is adopted, which is featured by combining both front/rear wheels as one wheel at the center of the front/rear axle [22]. This model is able to capture the primary dynamics of a vehicle, thus it has been widely used in motion planning problem formulations [23].

Suppose the cooperative lane change platoon consists of N_v CAVs. A 2-dimensional coordinated framework is set up as lane change scenario (Fig. 2). The following differential equations define the dynamics of CAV i ($i = 1, 2, ..., N_v$):

$$\frac{dx_i(t)}{dt} = v_i(t) \cdot \cos \theta_i(t) \tag{1a}$$

$$\frac{dy_i(t)}{dt} = v_i(t) \cdot \sin \theta_i(t) \tag{1b}$$

$$\frac{dv_i(t)}{dt} = a_i(t) \tag{1c}$$

$$\frac{da_i(t)}{dt} = jerk_i(t) \tag{1d}$$

$$\frac{d\theta_i(t)}{dt} = \frac{v_i(t) \cdot \tan \phi_i(t)}{L_w} \tag{1e}$$

$$\frac{d\phi_i(t)}{dt} = \omega_i(t) \tag{1f}$$

Herein, (x_i, y_i) denotes the coordinate of rear axle midpoint, v_i refers to the longitudinal velocity, a_i refers to the longitudinal acceleration, $jerk_i$ denotes the time derivative of acceleration,
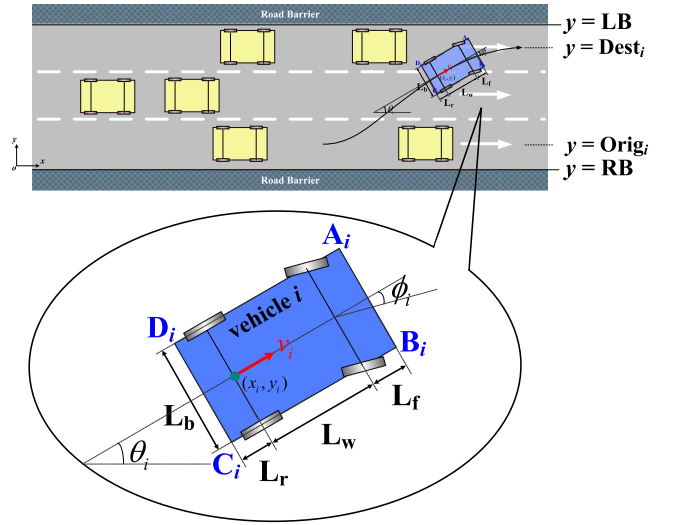

Fig. 2. Schematics on the CAV size, kinematics, and lane change scenario.

θ_i stands for the orientation angle, ϕ_i denotes the front-wheel steering angle, and ω_i is its time derivative. The geometric metrics include wheelbase L_w, front overhang length L_f, rear overhang length L_r, and vehicle width L_b (Fig. 2). In addition, the following constraints are imposed to ensure that the state/control variables are within admissible ranges:

$$|jerk_i(t)| \le \text{jerk}_{\max} \tag{2a}$$

$$|a_i(t)| \le a_{\max} \tag{2b}$$

$$0 \le v_i(t) \le v_{\max} \tag{2c}$$

$$|\theta_i(t)| \le \pi/2 \tag{2d}$$

$$|\phi_i(t)| \le \Phi_{\max} \tag{2e}$$

$$|\omega_i(t)| \le \Omega_{\max} \tag{2f}$$

Rapid changes of $a_i(t)$ or $\phi_i(t)$ lead to passenger discomfort [22], thus boundaries are imposed on $jerk_i(t)$ and $\omega_i(t)$; $|\theta_i(t)| \le \pi/2$ and $v_i(t) \ge 0$ forbid the driving movements in the opposite direction; the bounded constraints applied to $a_i(t)$ and $v_i(t)$ concern about safety; and $\phi_i(t)$ is mechanically limited.

Without exterior restrictions, (1) and (2) define how each CAV moves in the free space.

B. Scenario-Based Constraints

Apart from the kinematic constraints, scenario related constraints also have influences on the driving behaviors of the CAVs. The scenario related constraints aim to avoid two types of collisions, namely i) vehicle to vehicle collisions, and ii) vehicle to road barrier collisions.

Suppose that each vehicle is rectangular, and the road barriers are straight. The vehicle to road barrier collision is avoided if and only if the four corners of the vehicle do not hit the road barrier line. Herein, the four corner points of vehicle i (i.e., points A_i, B_i, C_i, and D_i as depicted in Fig. 2) are uniformly determined once x_i, y_i, and θ_i are specified ($i = 1, 2, ..., N_v$). Suppose the coordinates of the four corner points in the y axis are represented as y_{A_i}, y_{B_i}, y_{C_i}, and y_{D_i}, then the requirement that vehicle i hits neither left barrier $y = LB$ nor right barrier $y = RB$ is formulated as

$$RB \leq \Gamma \leq LB, \forall \Gamma \in \{y_{A_i}, y_{B_i}, y_{C_i}, y_{D_i}\}. \quad (3)$$

The collision-avoidance condition between two irregularly placed rectangles can be precisely described via a "triangle area criterion" [24]. With that criterion, the collision-avoidance constraints among all the CAVs are formulated as

$$S_{\triangle XA_iB_i} + S_{\triangle XB_iC_i} + S_{\triangle XC_iD_i} + S_{\triangle XD_iA_i} > S_{\square A_iB_iC_iD_i},$$
$$X \in \{A_k, B_k, C_k, D_k\}, i, k = 1, 2, ..., N_v, i \neq k, \quad (4)$$

where $S_\triangle$ denotes the triangle area, and $S_\square$ denotes the rectangle area.

C. Task-Related Constraints and Objective

The preceding sections have defined the kinematics and scenario related constraints. There are also task related constraints and an optimization objective, which are introduced as follows.

The goal of cooperative lane changes is to control the CAVs from the initial lanes to target lanes. Suppose the entire dynamic process begins from $t = 0$ and ends at $t = t_f$ (t_f is unknown *a priori*). At $t = 0$, the location of vehicle i (i.e., $[x_i(0), y_i(0)]$) is given. The other configuration variables are particularly required to satisfy

$$[v_i(0), a_i(0), jerk_i(0), \phi_i(0), \omega_i(0)] = [v_{st}, 0, 0, 0, 0], \quad (5)$$

where $v_{st} > 0$ denotes the consistent initial velocity for all of the vehicles. Eq. (5) is introduced here to avoid some corner cases, wherein two vehicles will *definitely* collide when $t > 0$, although no collision happens at $t = 0$. For example, at $t = 0$, two vehicles are driving on the same lane towards the same direction; the preceding vehicle's acceleration at $t = 0$ is 0, while the following vehicle's acceleration is positive; the two vehicles will collide right after $t = 0$ if their gap at $t = 0$ is sufficiently small. In this sense, (5) ensures that the dynamic process begins with a feasible state. Due to the same reason, the terminal configuration of CAV i is required as

$$[v_i(t_f), a_i(t_f), jerk_i(t_f), \phi_i(t_f), \omega_i(t_f)] = [v_{st}, 0, 0, 0, 0]. \quad (6)$$

Suppose vehicle i intends to change from lane $y = Orig_i$ to lane $y = Dest_i$ (Fig. 2), then

$$[y_i(0), \theta_i(0), y_i(t_f), \theta_i(t_f)] = [Orig_i, 0, Dest_i, 0]. \quad (7)$$

Remark 2.1: Eq. (7) is a unified formulation which enables non-adjacent lane changes. Moreover, $Dest_i = Orig_i$ implies that vehicle i intends to keep the original lane.

As a summary, the two-point boundary conditions (5)–(7) constitute the task-related constraints.

Besides that, a task-related criterion is needed to select a good solution among many feasible solutions. We choose minimization of completion time as the objective, because it can quantitatively differ simultaneous lane-change maneuvers from the sequential ones, thereby demonstrating the effectiveness of the cooperative scheme.

D. MVMP Problem Formulation

The elements introduced in the preceding sections formulate a centralized MVMP scheme in the form of a minimum-time optimal control problem P_0:

$$P_0:$$
$$\text{minimize } t_f$$
$$\text{s.t.} \quad \text{kinematics} - \text{based constraints } (1), (2);$$
$$\text{scenario} - \text{based constraints } (3), (4);$$
$$\text{task} - \text{related constraints } (5)-(7). \quad (8)$$

The unknowns in this problem include $x_i(t)$, $y_i(t)$, $\theta_i(t)$, $v_i(t)$, $a_i(t)$, $jerk_i(t)$, $\phi_i(t)$, $\omega_i(t)$, and t_f ($i = 1, 2, ..., N_v$). Herein, the decision variables are $jerk_i(t)$, $\omega_i(t)$, and t_f. The rest variables can be uniquely determined once the decision variables are specified. The details are introduced in the next section.

Remark 2.2: To solve (8), the main challenges originate from the large scale of the collision-avoidance constraints, and the high nonlinearity of the vehicle dynamics.

III. DECENTRALIZED MVMP METHOD

Since directly solving P_0 is difficult, we propose a two-stage MVMP method aiming to find near-optimal online solutions. For better understanding, the motivation is presented first, followed by the technical details. Finally, theoretical analyses are provided.

A. Motivation

Suppose there are two vehicles traveling towards the same direction but on two different lanes, and both vehicles intend to change to the other lane. If they implement the lane change maneuvers simultaneously without considering the potential collision, then they will definitely collide in the middle of the lane change process (Fig. 3(a)). If they could widen the rear-end gap before the lane changes, then the simultaneous lane changes will be naturally safe although both vehicles omit collision avoidance (Fig. 3(b)). This phenomenon implies that safety would be
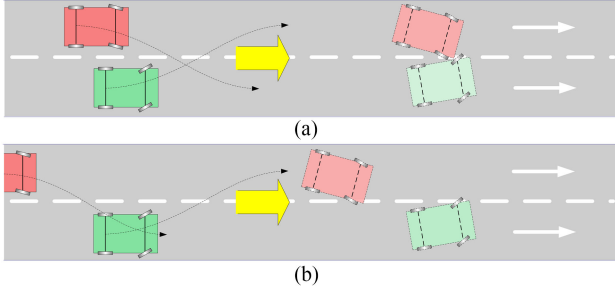
Fig. 3.   Schematics on a heuristic idea to achieve simultaneous lane changes: (a) the lane-change trajectories of both vehicles are conflicting; and (b) if the mutual gap is widened, then both vehicles can change lanes safely without concerns about inter-vehicle collisions.
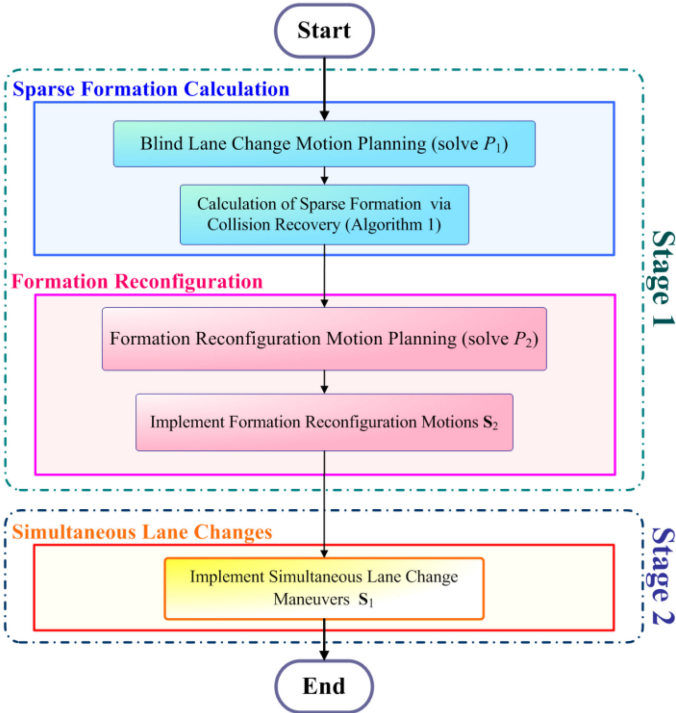

Fig. 4.   Flowchart of the proposed two-stage MVMP method.

implicitly ensured if the inter-vehicle distance is long enough before the simultaneous lane changes.

This idea inspires the authors to divide the entire lane-change process into two stages. At Stage 1, the vehicles do not change lanes; instead, they try to widen the inter-vehicle gaps via acceleration/deceleration. The gaps should be sufficiently large so that the vehicles, at Stage 2, can safely implement the simultaneous lane change maneuvers without the need to consider the collision avoidance constraints. In the rest of this paper, we use the term "sparse formation" to denote the large-gap platoon formation to be formed at the end of Stage 1.

To complete the cooperative lane changes in two stages, a few technical problems need to be solved: i) how to calculate the sparse formation; ii) how to control the CAV platoon to transfer to the sparse formation; and iii) how to control the CAVs to change the lanes simultaneously. A flowchart of the overall two-stage MVMP method is depicted in Fig. 4.
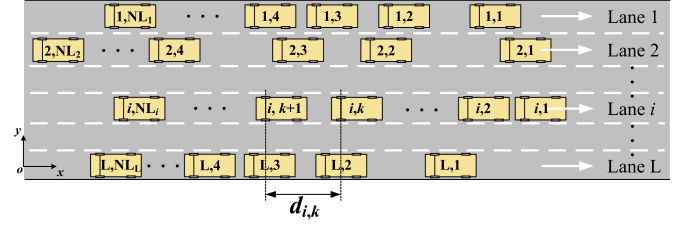

Fig. 5.   Schematics on the parametric notations related to lane classification at $t = 0$.

B. Sparse Formation Calculation

This section describes the generation of sparse formation. For the convenience of presentation, some notions are introduced first. Suppose that the road consists of L lanes, and lane i contains NL_i CAVs at $t = 0$. All the CAVs can be indexed by the lane number and its order in that lane. For example, $x_{i,j}$ denotes the x-axis coordinate of the jth vehicle in lane i (Fig. 5). Then we define

$$x_{i,k}(0) - x_{i,k+1}(0) = \mathrm{d}_{i,k}, i = 1,...,L, k = 1,...,\mathrm{NL}_i - 1, \tag{9}$$

where $\mathrm{d}_{i,k} \geq \mathrm{L}_r + \mathrm{L}_w + \mathrm{L}_f$. $\mathrm{d}_{i,k}$ measures the distance between adjacent vehicles k and $k + 1$ in the ith lane at $t = 0$. Suppose the sparse formation is reconfigured at $t = t_\zeta$. Then we define

$$x_{i,k}(t_\zeta) - x_{i,k+1}(t_\zeta) = \mathrm{d}_{i,k}^*, i = 1,...,L, k = 1,...,\mathrm{NL}_i - 1, \tag{10}$$

where $\{\mathrm{d}_{i,k}^*\}$ measures the distance between adjacent vehicles in each lane at $t = t_\zeta$. The goal of this section is to compute $\{\mathrm{d}_{i,k}^* | i = 1,...,L, k = 1,...,\mathrm{NL}_i - 1\}$.

The calculation of $\{\mathrm{d}_{i,k}^*\}$ consists of two steps. In the first step, the "blind" lane change motion of each CAV is derived. Herein, the blindness is reflected by the fact that each CAV changes the lane without concerning collisions with the other CAVs. Thereafter in the second step, the obtained blind lane change motions are checked for inter-vehicle collisions. If collisions happen, the gaps among the conflicting vehicles should be widened until the collisions can be completely avoided. This new formation is defined as the sparse formation. The remainder of this section introduces the two steps concretely.

1) Step 1: Blind Lane Change Motion Planning: This step aims to obtain the simultaneous lane change motions of the CAVs with collision-avoidance constraints completely ignored. A new problem P_1 is defined below:

$$P_1 :$$

$$\text{minimize } t_f$$

$$\text{s.t. Eqs.(1)} - (3) \text{ and } (5) - (7). \tag{11}$$

The optimal solution to P_1, denoted as $\mathbf{S}_1$, is recorded for future use. The approach to solve P_1 numerically is briefly introduced in Section III.E.

Remark 3.1: Compared with P_0, P_1 does not include (4), i.e., the high-dimensional collision-avoidance constraints among the vehicles, thus P_1 is far easier than P_0 to solve.

Algorithm 1: Calculation of $\{d_{i,k}^*\}$ via collision recovery.

1. Load $\mathbf{S}_1$;
2. Generate priority index set ψ;
3. **For** $n = 2 : N_v$, **do**
4.   Determine whether the trajectory of ψ_n collides with the trajectories of $\{\psi_1,...,\psi_{n-1}\}$;
5.   **While** collision exists, **do**
6.   Update the trajectories of vehicle ψ_n by a horizontal translation $|\Delta s|$ in the direction to widen the gap;
7.   Judge whether the updated trajectory of vehicle ψ_n collides to the trajectories of $\{\psi_1,...,\psi_{n-1}\}$ recorded in $\mathbf{S}_1$;
8.   **End while**
9.   Record the updated trajectory of vehicle $\{\psi_n\}$ in $\mathbf{S}_1$;
10. **End for**
11. Calculate $d_{i,k}^*$ according to (10) and $\mathbf{S}_1$;
12. Exit.

---

2) Step 2: Calculation of $\{d_{i,k}^*\}$ via Collision Recovery: Since inter-vehicle collisions are omitted in P_1, the obtained solutions are usually not collision-free. If $\mathbf{S}_1$ is a collision-free solution, then the original formation is regarded as the sparse formation, i.e., $\{d_{i,k}^*\} = \{d_{i,k}\}$. If $\mathbf{S}_1$ involves inter-vehicle collision(s), then this step introduces a collision recovery algorithm, which gradually widens the gaps among the conflicting vehicles until all collisions are avoided. Then the expanded formation determines $\{d_{i,k}^*\}$.

Priorities are assigned to all the N_v CAVs according to their x-axis coordinates at $t = 0$, and vehicle i with larger $x_i(0)$ gets higher priority. To record the priorities, an index set $\psi = \{\psi_1, \psi_2,..., \psi_{N_v}\}$ is utilized, wherein the element ψ_i denotes the vehicle with the ith highest priority. The vehicle with highest priority (i.e., vehicle ψ_1) changes lane as it plans in $\mathbf{S}_1$. Thereafter, whether vehicle ψ_2 is able to change its lane is measured by criterion (4) between ψ_2 and ψ_1. If the trajectory of vehicle ψ_2 does not collide with the trajectory of vehicle ψ_1 during $[0, t_\zeta]$, then vehicle ψ_2 can change lane as it plans in $\mathbf{S}_1$ as well; otherwise, the lane-change trajectory of vehicle ψ_2 should be horizontally translated for a unit distance $|\Delta s|$ to widen the gap, and the translated lane-change trajectory of vehicle ψ_2 is checked for collision with ψ_1 again. This translation-and-check loop is repeated until vehicle ψ_2 has no collision with vehicle ψ_1. Then, the final lane-change trajectory of vehicle ψ_2 replaces the original one recorded in $\mathbf{S}_1$. Following this strategy, ψ_3 yields its lane-change trajectory to avoid collisions with both vehicles ψ_1 and ψ_2, and finally the collision-free trajectory of vehicle ψ_3 replaces its original record in $\mathbf{S}_1$. As a general rule, vehicle ψ_i $(i > 1)$ should gradually yield its lane-change trajectory to the trajectories of vehicles $\{\psi_1,...,\psi_{i-1}\}$, until all conflicts are avoided. This process continues until all the vehicles have updated their lane-change trajectories in $\mathbf{S}_1$. The CAVs' initial locations in the current $\mathbf{S}_1$ form the desired sparse formation. Pseudo-code of the sparse formation calculation process is presented in Algorithm 1.

Remark 3.2: Through widening the inter-vehicle gaps, Algorithm 1 may enlarge the length of the platoon so as to form the sparse formation. As a reminder, Algorithm 1 may not be applicable to the road scenarios with additional platoon length related restrictions.

C. Formation Reconfiguration Motion Planning

If all the CAVs simultaneously begin their lane change maneuvers from the calculated sparse formation, then safety is naturally ensured. However, this is not true unless $\{d_{i,k}^*\} = \{d_{i,k}\}$. This section provides a bridge between $\{d_{i,k}\}$ and $\{d_{i,k}^*\}$, i.e., to control the CAV platoon from its original formation $\{d_{i,k}\}$ to the desired sparse formation $\{d_{i,k}^*\}$.

A formation reconfiguration scheme is defined as follows. Since the vehicles do not change lanes during this period, then

$$[\omega_i(t), \phi_i(t), \theta_i(t)] \equiv [0, 0, 0], t \in [0, t_\zeta], i = 1,..., N_v, \quad (12)$$

further reducing the kinematic system (1) to a longitudinal system:

$$\frac{dx_i(t)}{dt} = v_i(t) \tag{13a}$$

$$\frac{dy_i(t)}{dt} = 0 \tag{13b}$$

$$\frac{dv_i(t)}{dt} = a_i(t) \tag{13c}$$

$$\frac{da_i(t)}{dt} = jerk_i(t) \tag{13d}$$

Also, the collision-avoidance constraints (4) are reduced to

$$x_{i,k}(t) - x_{i,(k+1)}(t) \geq L_f + L_w + L_r, t \in [0, t_\zeta],$$
$$i = 1,..., L, k = 1,..., (NL_i - 1), \tag{14}$$

because only the adjacent vehicles in the same lane have collision possibilities. Similar with (6), the terminal states should be feasible, that is,

$$[v_i(t_\zeta), a_i(t_\zeta), jerk_i(t_\zeta)] = [v_{st}, 0, 0], i = 1, 2,..., N_v. \tag{15}$$

Then we formulate the formation reconfiguration scheme as

$$P_2:$$
$$\min\ t_\zeta$$
$$\text{s.t. Eqs. (2a), (2b), (2c), (5), (9), (10),}$$
$$\text{and (12)}-\text{(15).} \tag{16}$$

Remark 3.3: The scale of the collision-avoidance constraints (14) in P_2 grows linearly rather than exponentially with N_v; the kinematic constrains and collision constrains are linear. These factors make P_2 extremely easy to solve.

The solution to P_2 is recorded as $\mathbf{S}_2$. Through executing $\mathbf{S}_2$, the CAV platoon formation can be changed from $\{d_{i,k}\}$ to $\{d_{i,k}^*\}$.

D. Simultaneous Lane Changes

When the CAV platoon has reconfigured the formation from the original $\{d_{i,k}\}$ to $\{d^*_{i,k}\}$, the simultaneous lane change process begins immediately. This is achieved by implementing the updated $\mathbf{S}_1$ directly.

As a brief summary of the preceding sections, our proposed MVMP method i) manages to form a sparse platoon at the end of Stage 1 ($t = t_\zeta$), and ii) implements simultaneous lane changes at Stage 2 ($t \in [t_\zeta, t_\zeta + t_f)$). The technical procedures are outlined in Fig. 4.

Remark 3.4: In the proposed two-stage method, (4) is only utilized for judging the collisions in Algorithm 1, but not for constituting the collision avoidance constraints in P_1 or P_2. Therefore, the difficulties in directly handling P_0 are avoided using the proposed two-stage method.

E. Numerical Solutions to P_1 and P_2

The optimal control problems P_1 and P_2 are solved via the OCDT+IPM method, which utilizes orthogonal collocation direct transcription (OCDT) to discretize an optimal problem into an NLP, and then utilizes interior-point method (IPM) to address the NLP problem [25].

F. Theoretical Analysis

We now discuss some properties of the proposed MVMP method via the following lemmas and theorems.

Lemma 1: Stage 2 can be finished in finite time given any specified N_v.

Proof: Suppose it takes time Δt_i to finish the lane change of vehicle i ($i = 1,...,N_v$). Stage 2 finishes in $\max\{\Delta t_1,...,\Delta t_{N_v}\}$. As Δt_i is finite, $\max\{\Delta t_1,...,\Delta t_{N_v}\}$ is finite as well. ■

Remark 3.5: The number of the CAVs does not directly affect the time for lane changes, as all the vehicles act simultaneously. This is one important merit of the proposed MVMP method, that is, the time for lane changes is bounded and finite. On the contrary, for those methods where the lane changes take place sequentially, the total time increases as the number of lane-change vehicles increases.

Lemma 2: The length of lane-change path of vehicle i, denoted as $length_i$, is finite ($i = 1,...,N_v$).

Proof: Denote Δt as the simultaneous lane change completion time. Then,

$$|length_i| = \left| \int_{t=0}^{\Delta t} v_i(t) \cdot \cos\theta_i(t) \cdot dt \right| < v_{\max} \cdot \Delta t. \quad (17)$$

According to Lemma 1, $v_{\max} \cdot \Delta t$ is finite, rendering that $|length_i|$ is finite. ■

Lemma 3: The length of the sparse formation is finite.

Proof: Vehicle ψ_n will safely avoid collision with vehicle ψ_j ($j < n$), if the inter-vehicle gap between vehicle ψ_n and vehicle ψ_k ($\forall k, j \leq k < n$) is no less than $\sum_{ind=\psi_k}^{\psi_n} |length_{ind}|$ in the sparse formation. According to the definition of the sparse formation in Algorithm 1, $\sum_{ind=\psi_j}^{\psi_n} |length_{ind}|$ provides an upper bound of the inter-vehicle gap between vehicle ψ_n and vehicle
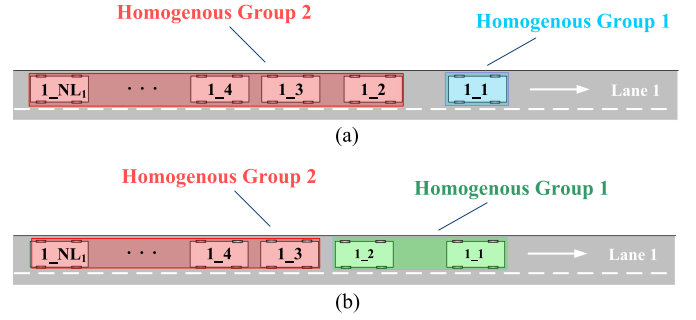

Fig. 6. Schematics on the analysis in Theorem 2: (a) gap adjustment process between vehicle 1_1 and 1_2; and (b) gap adjustment process between vehicle 1_2 and 1_3.

ψ_j. Through choosing $n = N_v$ and $j = 1$, an upper bound of the entire sparse formation length is $\sum_{ind=\psi_1}^{\psi_{N_v}} |length_{ind}|$, which is finite according to Lemma 2. Thus the length of the sparse formation is finite. ■

Theorem 1: Algorithm 1 is complete.

Proof: The proof process of Lemma 3 shows that each element in $\{d^*_{i,k}\}$ is finite. Thus each inner loop in Algorithm 1 can be finished within finite iterations. Thus Algorithm 1 can always provide solutions in finite time. ■

Theorem 2: The formation reconfiguration motion planning problem at Stage 1 is complete.

Proof: We can provide a specified type of solution to the concerned formation reconfiguration motion planning problem. Concretely, the inter-vehicle gap between each two vehicles is sequentially adjusted. At first, the gap between the first two vehicles in lane 1 (i.e., vehicles 1_1 and 1_2) is adjusted. To safely avoid collisions during the gap adjustment process, vehicles $1\_2, \ldots, 1\_NL_1$ are taken as a group, within which all the vehicles are considered to be homogenous in terms of the motion dynamics (Fig. 6(a)). Thereafter, the gap between vehicles 1_2 and 1_3 should be adjusted to the desired $d^*_{1,2}$. During that process, vehicles $1\_3, \ldots, 1\_NL_1$ are taken as one group, while vehicles 1_1 and 1_2 are taken as the other group (Fig. 6(b)). The vehicles in either group should move homogenously. This process iteratively continues until the last vehicle in the last lane has adjusted the gap. Suppose that each single gap adjustment process is finished in finite time, then the entire process can be finished in finite time. Although this specified type of solution appears clumsy, and it may not be the optimum one can derive from solving P_2, yet it is sufficient to show that the solution to P_2 exists. ■

Remark 3.6: The proof of Theorem 2 shows that the formation reconfiguration process at Stage 1 can be completed within finite time.

Theorem 3: The proposed two-stage MVMP method is complete.

Proof: Combining with Lemma 1, Theorems 2 and 3 can show that the proposed two-stage MVMP method is always able to provide solutions to a generic P_0, thus it is complete [26]. ■

Remark 3.7: Theorem 3 implies that feasible solutions to generic cooperative lane change MVMP problems P_0 always exist.

TABLE II
PARAMETRIC NOTATIONS AND SETTINGS

Parameter	Description	Setting
L_f	Vehicle front overhang length	0.960 m
L_w	Vehicle wheelbase	2.800 m
L_r	Vehicle rear overhang length	0.929 m
L_b	Vehicle width	1.942 m
LB	Left-barrier of road	5.625 m
UB	Right-barrier of road	-5.625 m
L	Number of lanes	3
N_v	Number of CAVs	20
v_{max}	Upper bound of $v_i(t)$, $i = 1, 2, ..., N_v$	15.0 m/s
Φ_{max}	Upper bound of $\lvert\phi_i(t)\rvert$, $i = 1, 2, ..., N_v$	0.576 rad
ω_{max}	Upper bound of $\lvert\omega_i(t)\rvert$, $i = 1, 2, ..., N_v$	0.3 rad/s
a_{max}	Upper bound of $\lvert a_i(t)\rvert$, $i = 1, 2, ..., N_v$	0.5 m/s^2
$jerk_{max}$	Upper bound of $\lvert jerk_i(t)\rvert$, $i = 1, 2, ..., N_v$	0.2 m/s^3
v_{st}	Consistent velocity of all the CAVs at the beginning/end of Stages 1 and 2	10.0 m/s
$\lvert\Delta s\rvert$	Unit horizontal translation distance in Algorithm 1	0.5 m
gap_{max}	Amplitude of the stochastic inter-vehicle gap	5 m

IV. SIMULATION RESULTS AND DISCUSSIONS

Simulations were performed in a mathematical programming language (AMPL) environment [27] and executed on an Intel Core i7-4710MQ CPU with 4 GB RAM that ran at 2.50 GHz. A software package of IPM, namely IPOPT, in the 3.12.4 version [28] was used with the default options.

Three-lane road scenario is considered in this work. The width of each lane is set to 3.75 m as a common global standard. The central lines of the lanes are $y = 3.75$, $y = 0$, and $y = -3.75$, respectively. Other parametric settings are listed in Table II.

In each simulation, randomly generated initial condition is considered. Herein, the randomness lies in i) before the lane changes, the number of CAVs running in each lane is randomly determined with equal probability; ii) the initial inter-vehicle gap between adjacent vehicles in each lane is uniformly distributed over $[0, gap_{max}]$, where gap_{max} refers to the amplitude; and iii) the target lane of each CAV is randomly determined with equal probability.

A video of the typical simulation results is provided at https://youtu.be/6jBFWLFb3A4.

A. Algorithm Efficiency

Recall that the proposed method requires online computation for i) solving P_1, ii) executing Algorithm 1, and iii) solving P_2, before the reconfiguration motions and the simultaneous lane change maneuvers are implemented. The first round of experiments investigates the online computational efficiency of the aforementioned three procedures with different settings of gap_{max}. To avoid getting biased results, each type of simulation was repeated 1,000 times with different random seeds. Fig. 7 demonstrates the comparative average CPU time. In general,
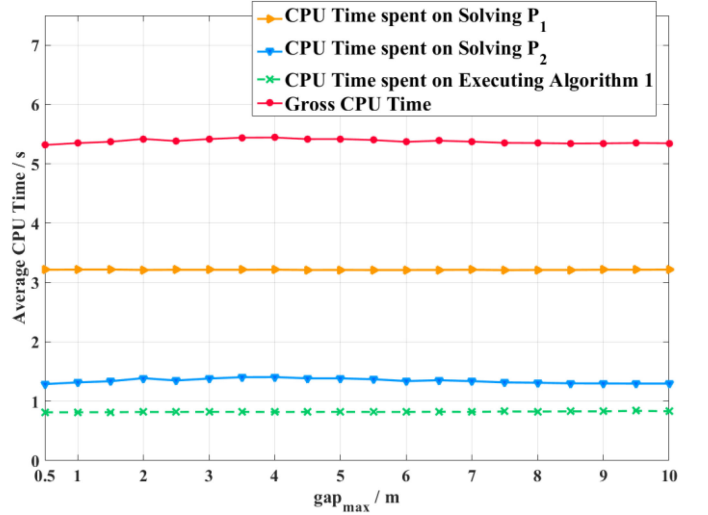

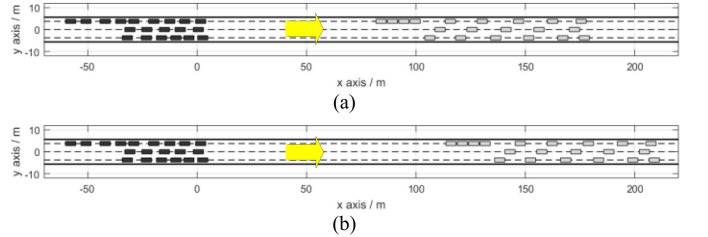Fig. 7. Comparative simulations on the CPU time with different settings of gap_{max}.

Fig. 8. Simulations on the formation reconfiguration process at Stage 1 with different settings of $jerk_{max}$: (a) $jerk_{max} = 0.2$, and (b) $jerk_{max} = 0.1$. Note that in Case (a) the completion time $t_\zeta = 17.53$ s while in Case (b) $t_\zeta = 20.66$ s.

the CPU time is nearly the same when gap_{max} varies, which indicates the proposed method performs insensitively to different traffic conditions, thus being unified. While waiting for the online computation results, each CAV has to cruise at the same speed v_{st}. As the computation process only takes a few seconds, the proposed method is suitable for the online applications.

The second round of experiments investigates the numerical solutions to P_1 and to P_2. Regarding the formation reconfiguration process, Fig. 8 shows one case with different settings of $jerk_{max}$. A smaller $jerk_{max}$ causes the acceleration and velocity profiles to change in a more gentle way, thus longer time is needed to reach the desired sparse formation (e.g., see Fig. 9). Fig. 10 shows the lane-change paths of one specified vehicle with different settings of ω_{max} or $jerk_{max}$. As ω_{max} decreases, the paths gradually become smoother, which can help alleviate the passengers' discomfort. A similar trend can be observed through decreasing $jerk_{max}$. The trends lie in the simulation results are reasonable, thus they show the unification capability of the proposed method in handling different constraints.

B. Comparisons on Solution Quality

This section evaluates the solution quality through conducting comparative experiments. As different methods are formulated based on different kinematic and scenario constraints, it is
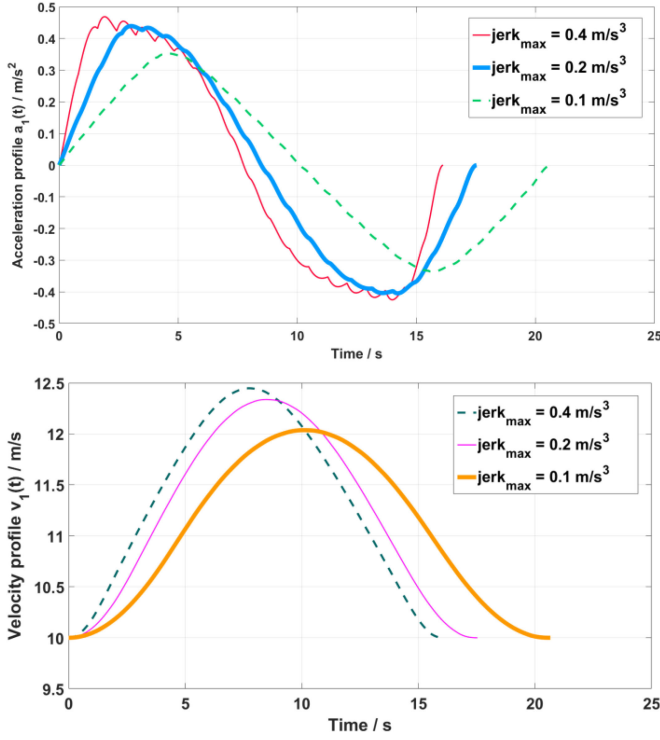
Fig. 9.   Obtained optimal acceleration and velocity profiles of vehicle 1 at Stage 1 with different settings of $\text{jerk}_{\max}$.
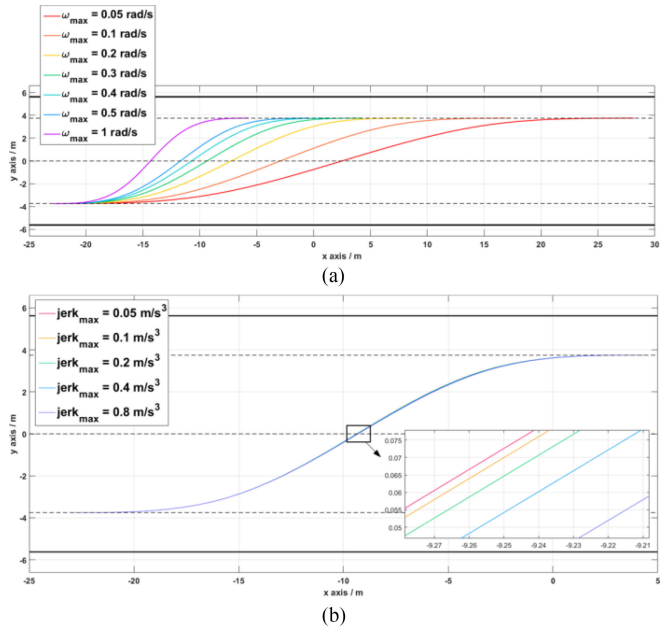

(a)

(b)

Fig. 10.   Comparative simulations on the lane change process at Stage 2 with different settings of (a) $\omega_{\max}$, and (b) $\text{jerk}_{\max}$. Note that the path of only one vehicle is the focus.

meaningless to make comparisons directly. Instead, we capture the typical features of several existing MVMP algorithms and summarize them into Algorithms 3–10 as listed in Table III. Three random cases are considered with $\text{gap}_{\max}$ equals to 2, 5, and 10, respectively. Table IV lists the obtained solution values, i.e., the lane change completion time.

TABLE III
DEFINITIONS OF COMPARATIVE MVMP ALGORITHMS

Name	Definition
Algorithm 2	The two-stage decentralized MVMP method proposed in this work
Algorithm 3	Same with Algorithm 2, except that the quintic polynomial based kinematics in [15] is adopted
Algorithm 4	Same with Algorithm 2, except that the envelope-based collision-avoidance condition in [20] is adopted
Algorithm 5	Same with Algorithm 2, except that the gap-based collision-avoidance condition in [15] is adopted
Algorithm 6	Same with Algorithm 2, except that the numerical solver is the ordinal optimization differential evolution algorithm in [16]
Algorithm 7	Same with Algorithm 2, except that the stage division strategy follows [17]
Algorithm 8	Same with Algorithm 2, except that the stage division strategy follows [19]
Algorithm 9	Same with Algorithm 2, except that the stage division strategy follows [21]
Algorithm 10	Solve (8) directly using OCDT+IPM [29]

TABLE IV
COMPARATIVE SIMULATION RESULTS ON SOLUTION QUALITY

Name	Case 1	Case 2	Case 3
Algorithm 2	21.822 s	19.958 s	17.366 s
Algorithm 3	22.854 s	20.972 s	18.373 s
Algorithm 4	52.965 s	49.919 s	52.443 s
Algorithm 5	62.269 s	61.280 s	59.658 s
Algorithm 6	N/A	N/A	N/A
Algorithm 7	104.780 s	113.580 s	83.942 s
Algorithm 8	36.241 s	32.924 s	34.540 s
Algorithm 9	28.550 s	31.835 s	33.238 s
Algorithm 10	16.531 s	16.094 s	9.885 s

Algorithm 3 represents those methods with indirect kinematic models. Compared to the results of Algorithm 2, using quantic polynomials to describe the lane-change trajectories renders more computation time, because the kinematic flexibility is limited by this fixed polynomial structure. Algorithms 4 and 5 represent those methods with incomplete collision-avoidance models. Both algorithms perform poorly especially when the initial formation is compact, because the collision-avoidance conditions are overly conservative. Algorithm 6 is inefficient because the involved stochastic optimizer (differential evolution algorithm) is not able to precisely tackle the path constraints in either P_1 or P_2. Algorithm 7 or 8 applies sequential lane changes. Concretely, Algorithm 7 requires the vehicles to change lane one after another, while Algorithm 8 requires the vehicles with the same target lane should change lanes simultaneously. Algorithm 7 is purely a sequential planner whereas Algorithm 8 conducts simultaneous planning in part, thus the results derived by Algorithm 8 are better than those of Algorithm 7. Algorithm 9 considers formulating a standard formation before the simultaneous lane change stage. The results obtained via Algorithm 9 are no better than those of Algorithm 2, because time has been wasted in forming a standard formation. Algorithm 10 aims to provide the optimal solution to the centralized problem P_0 in each case. Although the solutions derived from Algorithm 2 are

worse than the optima derived from Algorithm 10, Algorithm 2 universally strikes a balance between task completion time and CPU time when gap_{max} varies.

V. CONCLUSION

A two-stage multi-vehicle motion planning (MVMP) method has been proposed for cooperative lane changes among connected and automated vehicles (CAVs). At Stage 1, a sufficiently sparse formation is reconfigured so that all the vehicles, at Stage 2, can simultaneously change the lanes with collision avoidance implicitly ensured. Theoretical analyses have shown the completeness of the method. Furthermore, simulation results indicate that the proposed method i) is suitable for online decision making, ii) performs consistently in handling various constraints, and iii) strikes a balance between CPU time and task completion time.

As our future works, mixed-traffic scenario with non-CAVs will be investigated. Furthermore, cases on how to efficiently divide the whole CAV platoon into isolated subgroups when the road space is limited will also be considered.

ACKNOWLEDGMENTS

REFERENCES

[1] J. Rios-Torres and A. A. Malikopoulos, "A survey on the coordination of connected and automated vehicles at intersections and merging at highway on-ramps," *IEEE Trans. Intell. Transp. Syst.*, vol. 18, no. 5, pp. 1066–1077, May 2017.

[2] E. Moradi-Pari, H. N. Mahjoub, H. Kazemi, Y. P. Fallah, and A. Tahmasbi-Sarvestani, "Utilizing model-based communication and control for cooperative automated vehicle applications," *IEEE Trans. Intell. Veh.*, vol. 2, no. 1, pp. 38–51, Mar. 2017.

[3] C. Katrakazas, M. Quddus, W. H. Chen, and L. Deka, "Real-time motion planning methods for autonomous on-road driving: State-of-the-art and future research directions," *Transp. Res. Part C: Emerg. Technol.*, vol. 60, pp. 416–442, 2015.

[4] B. Paden, M. Čáp, S. Z. Yong, D. Yershov, and E. Frazzoli, "A survey of motion planning and control techniques for self-driving urban vehicles," *IEEE Trans. Intell. Veh.*, vol. 1, no. 1, pp. 33–55, Mar. 2016.

[5] M. Chen, J. F. Fisac, S. Sastry, and C. J. Tomlin, "Safe sequential path planning of multivehicle systems via double-obstacle Hamilton-Jacobi Isaacs variational inequality," in *Proc. Eur. Control Conf.*, 2015, pp. 3304–3309.

[6] M. During and K. Lemmer, "Cooperative maneuver planning for cooperative driving," *IEEE Intell. Transp. Syst. Mag.*, vol. 8, no. 3, pp. 8–22, Fall 2016.

[7] B. Li, Y. M. Zhang, Z. Shao, and N. Jia, "Simultaneous versus joint computing: A case study of multivehicle parking motion planning," *J. Comput. Sci.*, vol. 20, pp. 30–40, 2017.

[8] D. Bevly *et al.*, "Lane change and merge maneuvers for connected and automated vehicles: A survey," *IEEE Trans. Intell. Veh.*, vol. 1, no. 1, pp. 105–120, Mar. 2016.

[9] B. Li *et al.*, "Paving green passage for emergency vehicle in heavy traffic: Real-time motion planning under the connected and automated vehicles environment," in *Proc. IEEE Int. Symp. Safety, Security Rescue Robot.*, 2017, pp. 153–158.

[10] J. E. Naranjo, C. Gonzalez, R. Garcia, and T. De Pedro, "Lane-change fuzzy control in autonomous vehicles for the overtaking maneuver," *IEEE Trans. Intell. Transp. Syst.*, vol. 9, no. 3, pp. 438–450, Sep. 2008.

[11] C. Bax, P. Leroy, and M. P. Hagenzieker, "Road safety knowledge and policy: A historical institutional analysis of the Netherlands," *Transp. Res. Part F: Traffic Psychol. Behav.*, vol. 25, pp. 127–136, 2014.

[12] F. You, R. Zhang, G. Lie, H. Wang, H. Wen, and J. Xu, "Trajectory planning and tracking control for autonomous lane change maneuver based on the cooperative vehicle infrastructure system," *Expert Syst. Appl.*, vol. 42, no. 14, pp. 5932–5946, 2015.

[13] E. Ward, N. Evestedt, D. Axehill, and J. Folkesson, "Probabilistic model for interaction aware planning in merge scenarios," *IEEE Trans. Intell. Veh.*, vol. 2, no. 2, pp. 133–146, Jun. 2017.

[14] J. Nilsson, J. Silvlin, M. Brannstrom, E. Coelingh, and J. Fredriksson, "If, when, and how to perform lane change maneuvers on highways," *IEEE Intell. Transp. Syst. Mag.*, vol. 8, no. 4, pp. 68–78, Winter 2016.

[15] Y. Luo, Y. Xiang, K. Cao, and K. Li, "A dynamic automated lane change maneuver based on vehicle-to-vehicle communication," *Transp. Res. Part C: Emerg. Technol.*, vol. 62, pp. 87–102, 2016.

[16] X. Fu, Y. Jiang, D. Huang, K. Huang, and J. Wang, "Trajectory planning for automated driving based on ordinal optimization," *Tsinghua Sci. Technol.*, vol. 22, no. 1, pp. 62–72, 2017.

[17] M. Atagoziyev, K. W. Schmidt, and E. G. Schmidt, "Lane change scheduling for autonomous vehicles," *IFAC-PapersOnLine*, vol. 49, no. 3, pp. 61–66, 2016.

[18] S. Samiee, S. Azadi, R. Kazemi, A. Eichberger, B. Rogic, and M. Semmer, "Performance evaluation of a novel vehicle collision avoidance lane change algorithm," in *Advanced Microsystems for Automotive Applications 2015*. New York, NY, USA: Springer-Verlag, 2016, pp. 103–116.

[19] D. Desiraju, T. Chantem, and K. Heaslip, "Minimizing the disruption of traffic flow of automated vehicles during lane changes," *IEEE Trans. Intell. Transp. Syst.*, vol. 16, no. 3, pp. 1249–1258, Jun. 2015.

[20] J. Suh, B. Kim, and K. Yi, "Stochastic predictive control based motion planning for lane change decision using a vehicle traffic simulator," in *Proc. IEEE Conf. Expo Transp. Electrification Asia-Pac.*, 2016, pp. 900–907.

[21] B. Li, Y. M. Zhang, Y. Ge, Z. Shao, and P. Li, "Optimal control-based online maneuver planning for cooperative lane change of connected and automated vehicles," in *Proc. IEEE/RSJ Int. Conf. Intell. Robots Syst.*, 2017, pp. 3689–3694.

[22] B. Li, K. Wang, and Z. Shao, "Time-optimal maneuver planning in automatic parallel parking using a simultaneous dynamic optimization approach," *IEEE Trans. Intell. Transp. Syst.*, vol. 17, no. 11, pp. 3263–3274, Nov. 2016.

[23] L. Ma, J. Xue, K. Kawabata, J. Zhu, C. Ma, and N. Zheng, "Efficient sampling-based motion planning for on-road autonomous driving," *IEEE Trans. Intell. Transp. Syst.*, vol. 16, no. 4, pp. 1961–1976, Aug. 2015.

[24] B. Li and Z. Shao, "A unified motion planning method for parking an autonomous vehicle in the presence of irregularly placed obstacles," *Knowl.-Based Syst.*, vol. 86, pp. 11–20, 2015.

[25] B. Li, H. Liu, D. Xiao, G. Yu, and Y. M. Zhang, "Centralized and optimal motion planning for large-scale AGV systems: A generic approach," *Adv. Eng. Softw.*, vol. 106, pp. 33–46, 2017.

[26] M. N. Pivtoraiko, "Differentially constrained motion planning with state lattice motion primitives," Ph.D. dissertation, Robotics Inst., Carnegie-Mellon Univ., Pittsburgh, PA, USA, 2012.

[27] R. Fourer, D. Gay, and B. Kernighan, *AMPL: A Modeling Language for Mathematical Programming*. Pacific Grove, CA, USA: Brooks/Cole, 2003.

[28] A. Wächter and L. T. Biegler, "On the implementation of an interior-point filter line-search algorithm for large-scale nonlinear programming," *Math. Programm.*, vol. 106, no. 1, pp. 25–57, 2006.

[29] B. Li, Z. Shao, Y. M. Zhang, and P. Li, "Nonlinear programming for multivehicle motion planning with Homotopy initialization strategies," in *Proc. 13th IEEE Conf. Autom. Sci. Eng.*, 2017, pp. 118–123.
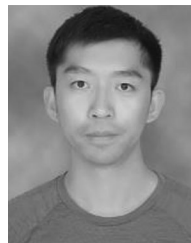
Bai Li (S'14) received the B.S. degree from the School of Advanced Engineering, Beijing University of Aeronautics and Astronautics, Beijing, China, in 2013. Since September 2013, he has been working toward the Ph.D. degree with the College of Control Science and Engineering, Zhejiang University, Hangzhou, China. From November 2016 to June 2017, he visited the Department of Civil and Environmental Engineering, University of Michigan, Ann Arbor, USA, as a joint training Ph.D. student. His research interests include motion planning and control methods for connected and automated vehicles. He was a recipient of the 2017 Best Paper Prize for *International Federation of Automatic Control* Journals (*Engineering Applications of Artificial Intelligence*).

Youmin Zhang (M'99–SM'07) received the B.S., M.S., and Ph.D. degrees from the Department of Automatic Control, Northwestern Polytechnical University, Xi'an, China, in 1983, 1986, and 1995, respectively. He is a Professor with the Department of Mechanical, Industrial and Aerospace Engineering, Concordia University, Montreal, QC, Canada. He held also several teaching and research positions previously in Northwestern Polytechnical University, University of New Orleans, Louisiana State University, State University of New York at Binghamton, The University of Western Ontario, and Aalborg University, respectively. He has published 4 books, more than 460 journal and conference papers, and book chapters.

Yiheng Feng received the B.S. and M.E. degrees from the Department of Control Science and Engineering, Zhejiang University, Hangzhou, China, in 2005 and 2007, respectively, the master's degree from the Civil Engineering Department, University of Minnesota, Twin Cities, Minneapolis, MN, USA, in 2011, and the Ph.D. degree in systems and industrial engineering from the University of Arizona, Tucson, Arizona, in 2015. He is currently an Assistant Research Scientist with the University of Michigan Transportation Research Institute, Ann Arbor, MI, USA. His research interests include traffic signal systems, connected and automated vehicles, arterial performance measurement, and travel demand modeling.

Yue Zhang (S'15) received the B.S. degree in electronics and information engineering from the Huazhong University of Science and Technology, Wuhan, China, in 2013. She is currently working toward the Ph.D. degree with the Division of Systems Engineering, Boston University, Boston, MA, USA. During the summer of 2015, she was a Research Intern with the National Transportation Research Center, the Oak Ridge National Laboratory, Oak Ridge, TN, USA. Her research interests include discrete event systems and optimal control of hybrid systems, with applications to intelligent transportation systems.

Yuming Ge received the B.S. degree in communication engineering from the Beijing University of Posts and Telecommunications, Beijing, China, and the Ph.D. degree from the Institute of Computing Technology, Chinese Academy of Science, Beijing, China. He is currently a Senior Engineer with the China Academy of Information and Communications Technology, Beijing, China. From December 2016 to March 2017, he visited the University of Michigan Transportation Research Institute as a Visiting Scholar. His research interests include standardization, innovation research, and international cooperation in the area of connected and automated vehicles, especially V2X communications, cybersecurity, and data analysis.

Zhijiang Shao received the B.S. degree from the Department of Chemical Engineering, Zhejiang University, Hangzhou, China, in 1992, and the Ph.D. degree from the College of Control Science and Engineering, Zhejiang University, in 1997. He was a Lecturer with Zhejiang University from 1997 to 1999, and an Associate Professor from 1999 to 2004. Since 2004, he has been a Professor with the same university. His research interests include the numerical solvers for large-scale dynamic optimization problems.